JOURNAL OF VIROLOGY, Dec. 2004, p. 13755–13768 Vol. 78, No. 24
0022-538X/04/$08.00+0 DOI: 10.1128/JVI.78.24.13755–13768.2004

Glycocalyx Restricts Adenoviral Vector Access to Apical Receptors Expressed on Respiratory Epithelium In Vitro and In Vivo: Role for Tethered Mucins as Barriers to Lumenal Infection

Jaclyn R. Stonebraker,[1] Danielle Wagner,[1] Robert W. Lefensty,[1] Kimberlie Burns,[1] Sandra J. Gendler,[2] Jeffrey M. Bergelson,[3] Richard C. Boucher,[1] Wanda K. O'Neal,[1] and Raymond J. Pickles[1,4]*

Cystic Fibrosis/Pulmonary Research and Treatment Center[1] and Department of Microbiology and Immunology,[4] University of North Carolina at Chapel Hill, Chapel Hill, North Carolina; Mayo Clinic Scottsdale, Scottsdale, Arizona[2]; and Division of Immunologic and Infectious Diseases, Children's Hospital of Philadelphia, Philadelphia, Pennsylvania[3]

Received 16 March 2004/Accepted 30 July 2004

Inefficient adenoviral vector (AdV)-mediated gene transfer to the ciliated respiratory epithelium has hindered gene transfer strategies for the treatment of cystic fibrosis lung disease. In part, the inefficiency is due to an absence of the coxsackie B and adenovirus type 2 and 5 receptor (CAR) from the apical membranes of polarized epithelia. In this study, using an in vitro model of human ciliated airway epithelium, we show that providing a glycosylphosphatidylinositol (GPI)-linked AdV receptor (GPI-CAR) at the apical surface did not significantly improve AdV gene transfer efficiency because the lumenal surface glycocalyx limited the access of AdV to apical GPI-CAR. The highly glycosylated tethered mucins were considered to be significant glycocalyx components that restricted AdV access because proteolytic digestion and inhibitors of O-linked glycosylation enhanced AdV gene transfer. To determine whether these in vitro observations are relevant to the in vivo situation, we generated transgenic mice expressing GPI-CAR at the surface of the airway epithelium, crossbred these mice with mice that were genetically devoid of tethered mucin type 1 (Muc1), and tested the efficiency of gene transfer to murine airways expressing apical GPI-human CAR (GPI-hCAR) in the presence and absence of Muc1. We determined that AdV gene transfer to the murine airway epithelium was inefficient even in GPI-hCAR transgenic mice but that the gene transfer efficiency improved in the absence of Muc1. However, the inability to achieve a high gene transfer efficiency, even in mice with a deletion of Muc1, suggested that other glycocalyx components, possibly other tethered mucin types, also provide a significant barrier to AdV interacting with the airway lumenal surface.

Replication-deficient adenoviral vectors (AdV) based on serotypes 2 and 5 have been shown to efficiently transduce nonpolarized human airway epithelial cells in vitro. However, these vectors have failed to efficiently transfer transgenes to the human differentiated mucociliary respiratory epithelium after intralumenal delivery in vitro and in vivo (26, 28, 36, 46, 47). For cystic fibrosis (CF) lung gene therapy, the target airway epithelial cells requiring expression of a functional CF transmembrane conductance regulator (CFTR) are considered the ciliated airway epithelial cells (7). Clinical and preclinical studies of AdV-mediated gene transfer to the lung epithelium have concluded that the numbers of epithelial cells expressing the corrective transgene, CFTR, have been low and insufficient for correction of the CF ion transport defect in the lungs (19, 21). In addition, immune responses to expressed viral genes and/or transgenes combined with the involvement of inflammatory cells such as macrophages limit the level and duration of transgene expression by AdV (11, 33, 42, 43, 49). These observations have limited the utility of AdV-based gene transfer strategies for CF lung disease.

Inefficient AdV-mediated gene transfer via the lumenal surfaces of polarized epithelial cells has been reported to be due to the absence of apical receptors which are required for Ad entry (28, 36). The attachment receptor for human Ad from subgroups A, C, D, E, and F is the coxsackie B and adenovirus type 2 and 5 receptor (CAR) (4, 32). Cell lines that are normally resistant to Ad infection with these serotypes become permissive for infection when transfected with human CAR (hCAR), suggesting that hCAR alone is sufficient to mediate the entry of Ad into cells (4, 27, 32, 37). Most polarized epithelial cells, including human columnar airway epithelial cells, express hCAR at the basolateral surface, with undetectable hCAR at the apical surface (28, 36). The localization of hCAR to regions associated with tight junctional complexes and the suggestion that hCAR-hCAR interactions may be an important mechanism of cell-cell adhesion in these regions have led to the speculation that the natural spread of Ad infection in the lung may involve a disruption of hCAR-mediated cell adhesion (15, 35). In contrast to columnar cells, airway epithelial basal cell types express hCAR with a nonpolarized distribution and are efficiently infected by AdV delivered to the basolateral

* Corresponding author. Mailing address: CF/Pulmonary Research and Treatment Center, University of North Carolina at Chapel Hill, 7021 Thurston Bowles, Chapel Hill, NC 27759-7248. Phone: (919) 966-1522. Fax: (919) 966-5178. E-mail: branston@med.unc.edu.

compartments of human polarized airway epithelial cell cultures (28, 48).

Several strategies to retarget AdV to receptors present on the airway surface have been attempted to improve gene transfer efficiency to the respiratory epithelium. Although targeted vectors have shown promise with nonpolarized cell lines expressing target receptors, only modest improvements in gene transfer efficiency to well-differentiated respiratory epithelia have been reported (18, 22). The feasibility of targeting AdV to the apical surfaces of polarized epithelia was previously tested by redirecting hCAR to the apical membrane by engineering the external domain of hCAR (containing the Ad binding domain) to the glycosylphosphatidylinositol (GPI) linker region of CD55, generating a GPI-hCAR chimera (27, 37). On nonpolarized cells, hCAR and GPI-hCAR are equally efficient at mediating AdV attachment and entry (27, 37). Although the transfection of GPI-hCAR into polarized MDCK cells led to an apical distribution of GPI-hCAR, a significant enhancement of AdV-mediated gene transfer after apical inoculation was not observed. However, increased AdV access to GPI-hCAR and a significant improvement in gene transfer efficiency were achieved after neuraminidase (NA) treatment of the apical surfaces of MDCK-GPI-hCAR cells, suggesting that apical surface sialic acid residues contained within the glycocalyx layer of MDCK cells restricted AdV access to GPI-hCAR (27). In contrast, in an in vitro model of human differentiated airway epithelium, apical GPI-hCAR expression was sufficient to mediate efficient gene transfer, and the access of AdV to apical GPI-hCAR was unhindered by glycocalyx components (37).

To resolve these discrepancies, in addition to expressing GPI-hCAR in an in vitro model of human tracheobronchial airway epithelium (HAE) that recapitulates the polarized, pseudostratified mucociliary epithelium present in human cartilaginous airways in vivo, we also generated transgenic mice expressing GPI-hCAR with an epithelial cell-specific distribution and used this model to determine if AdV-mediated gene transfer efficiency is enhanced by the presence of an apical AdV receptor in the murine airway epithelium in vivo. Since previous studies have shown that transfection of the large, heavily glycosylated tethered mucin MUC1 into nonpolarized human airway epithelial cells or MDCK cells reduces AdV-mediated gene transfer efficiency (1), we also used a combination of Muc1 knockout (30) and GPI-hCAR transgenic mouse models to determine the role of this specific mucin on AdV access to apical GPI-hCAR in vivo.

MATERIALS AND METHODS

Cell culture. Human airway tracheobronchial epithelial cells were obtained from airway specimens that were resected during lung transplantation according to UNC Institutional Review Board (IRB)-approved protocols by the UNC CF Center Tissue Culture Core and then cultured as previously described (28). Briefly, primary cells derived from single patient sources were expanded on plastic to generate passage 1 (P1) cells and were plated at a density of 250,000 cells per well on permeable Transwell-Col (T-Col; 12-mm diameter) supports. HAE cultures were grown with an air-liquid interface for 4 to 6 weeks to generate well-differentiated, polarized cultures that resembled in vivo pseudostratified mucociliary epithelium.

For the generation of HAE cultures expressing GPI-hCAR (GPI-hCAR HAE), the apical surfaces were exposed to sodium caprate (30 mM in tissue culture medium for 3 min to transiently open epithelial cell tight junctions and expose basolateral surfaces to facilitate AdV uptake), rinsed three times with phosphate-buffered saline (PBS), and then inoculated with AdV expressing GPI-hCAR (AdVgpi-hCAR; 2×10^{10} particles/ml in 0.3 ml of medium for 4 h at 37°C). Forty-eight hours later, GPI-hCAR was assessed by immunofluorescence by incubating the lumenal surfaces of HAE cells with an anti-human CAR monoclonal mouse antibody (RmcB) followed by anti-mouse immunoglobulin G (IgG)-Texas Red. Fluorescence microscopy was performed en face with a Leica Leitz DMIRB inverted fluorescence microscope equipped with a cooled color charge-coupled device digital camera (Q-Imaging; MicroPublisher). Confocal XZ optical sectioning was performed with a laser scanning confocal microscope (Leica TCS). For immunogold localization, identical procedures were performed except that goat anti-mouse IgG conjugated to 12-nm-diameter colloidal gold particles was use as the secondary antibody (Jackson Labs). Colloidal gold was visualized by standard transmission electron microscopy.

Adenoviral vectors. Adenoviral vectors containing the green fluorescent protein (GFP) gene (AdVGFP), the β-galactosidase (LacZ) gene (AdVLacZ), and the GPI-hCAR chimeric gene (AdVgpi-hCAR) under the control of a cytomegalovirus promoter were all produced by the UNC Gene Therapy Center Vector Core. The GPI-hCAR construct was generated as previously described (27).

Generation of mouse models. Transgenic mice were generated and utilized with approval from the UNC Institutional Animal Care and Use Committee. For epithelial cell-specific expression, the K18 promoter element from plasmid K18mTELacZ (a kind gift from Jim Hu [12, 13]), which was shown to direct epithelial cell-specific expression in transgenic mice, was fused to the GPI-hCAR sequence by a PCR-based cloning strategy (details available upon request). The polyadenylation signal was originally derived from pEGFP-C1 (Clontech). Although the K18 promoter element was shown to direct expression to the epithelium in transgenic mice, there was a vast difference from founder line to founder line in previous reports, suggesting that this promoter is subject to positional effects (12, 13). In order to reduce the likelihood of positional effects and to increase the chances of obtaining the desired expression pattern, we used insulator elements from the chicken β-actin gene (a kind gift from Gary Felsenfeld [14, 39]), which have been shown to reduce positional effects in transgenic models, to flank the entire expression cassette. Pronuclear injections of a transgenic construct containing the insulator elements, the K18 epithelial cell-specific promoter, and the GPI-hCAR sequence into C57BL/6J × C3H mouse strain blastocysts were performed in the UNC Transgenic Core Facility according to established protocols. Founder animals that transmitted GPI-hCAR to their progeny were identified by Southern blotting (not shown), and progeny mice (identified by PCR; details available upon request) were evaluated for the expression of GPI-hCAR.

For immunolocalization of GPI-hCAR in murine tissue, tissues were fixed in Omnifix II (FR Chemicals, Albany, N.Y.), and sections of paraffin-embedded tissues were prepared. After rehydration, tissue sections were probed with an anti-human CAR antibody (RmcB) followed by goat anti-mouse IgG conjugated to fluorescein isothiocyanate (Jackson Labs). Muc1 immunolocalization was performed as described above except that tissues were incubated with an Armenian hamster monoclonal anti-Muc1 antibody (CT2) (17) followed by goat anti-Armenian hamster IgG conjugated to Texas Red (Jackson Labs). For immunogold detection in murine tracheas, isolated tracheas were incubated with RmcB followed by goat anti-mouse IgG conjugated to 12-nm-diameter colloidal gold particles. The investigator performing the immunolocalization was blinded to the genotypes of the animals under study.

Assessment of gene transfer. For assessments of AdV-mediated gene transfer to HAE and GPI-hCAR HAE, 72 h after sodium caprate or sodium caprate-AdVgpihCAR inoculation the lumenal surfaces of the cultures were rinsed with PBS and inoculated with AdVGFP or AdVLacZ (2×10^{10} particles/ml in 0.3 ml of medium for 2 h at 37°C; $\sim 4 \times 10^4$ particles per cell [PPC], unless otherwise stated). Forty-eight hours later, the gene transfer efficiency was assessed either by image analyses of GFP expression that quantitated the percentage of apical surface area expressing the transgene or by standard enzyme assays for AdVLacZ as described previously (28, 48).

Delivery of AdV to the murine tracheal epithelium was performed with anesthetized animals in which a double tracheostomy was performed between the third and sixth tracheal cartilage rings. This technique allowed for the animals to breathe spontaneously through the distal tracheostomy while AdVLacZ was delivered by a catheter through the proximal tracheostomy. AdVLacZ (20 μl of 10^{11} particles/ml; $\sim 4 \times 10^4$ PPC) was delivered with direct visualization to the region of the murine tracheal epithelium in between the tracheostomies (~ 0.1 cm^2 of epithelial surface area) and was maintained for a 30-min incubation. For experiments with sodium caprate pretreatment, the murine tracheal epithelium was instilled with sodium caprate (25 mM for 5 min) and the tracheal lumens were rinsed with PBS immediately prior to AdVLacZ inoculation. All procedures were performed according to protocols approved by the UNC Institutional Animal Care and Use Committee. Forty-eight hours after AdVLacZ inoculation,

the tracheas were removed, dissected longitudinally, and stained for LacZ expression by standard X-Gal (5-bromo-4-chloro-3-indolyl-β-D-galactopyranoside) procedures as described previously (26). Digital images of the stained tracheas were obtained, and the percentages of epithelial surface area that were positive for transgene expression were determined by digital morphometry (Adobe Photoshop) of the tracheal epithelial surface. For all experiments, the investigators performing the inoculations and/or digital morphometry were blinded to the genotypes of the animals until after data analyses were performed. Statistics were performed with Student's *t* test by the use of SigmaStat software.

Detection of apical surface glycocalyx components. Identifications of glycocalyx components were performed with three or more different patient sources of cells, but estimates of relative amounts of particular antigens were compared for a single patient source. Lectin and antibody detection techniques were used to determine the absence or presence of the following specific moieties: α2-3-linked sialic acid residues (MAL II lectin; Vector Labs), α2-6-linked sialic acid residues (SNA lectin; Vector Labs), MUC1 (b2729 antibody; a gift from Fujirebio Diagnostics Inc.), heparan sulfate (F58-10E4, F69-3G10, or HepSS-1 antibody; Seikagaku), chondroitin-4-sulfate and chondrotin-6-sulfate (MC21C and LY11 antibodies, respectively; Seikagaku), and keratan sulfate (5D4 antibody; Seikagaku). Lectins and primary antibodies were incubated with the apical surfaces of live or paraformaldehyde-fixed HAE followed by incubation with secondary reagents conjugated to Cy3 or Texas Red.

RT-PCR for mucin gene expression. The expression of a variety of reported transmembrane mucins was determined for human and mouse airway tissues by reverse transcription-PCR (RT-PCR) analysis. For all mucins, primers were designed from National Center for Biotechnology Information accession numbers (reference sequence numbers when available) to span at least one intron (primers and accession numbers are available upon request). Based upon expression information in Unigene (National Center for Biotechnology Information), all reported transmembrane mucins are expressed in the placenta and/or the colon, so these two tissues were chosen as positive controls (human colon and placental RNAs were purchased from Ambion; mouse colon RNAs were isolated in-house). Human primary bronchial RNAs were isolated from HAE and nasal RNAs were isolated from epithelial cells obtained via nasal scrape biopsies according to established IRB-approved protocols. Mouse tracheal and lung RNAs were isolated from dissected mouse tissues. RNAs from all samples prepared in-house were purified by the use of RNeasy RNA Mini isolation kits (Qiagen) followed by DNase digestion (Qiagen). Two hundred nanograms of total RNA was reverse transcribed to cDNA by the use of random primers and SuperScript II reverse transcriptase (Invitrogen). PCRs were performed with AmpliTaq Gold *Taq* polymerase (Applied Biosystems) in the buffer supplied by the manufacturer, with 10 pmol of each primer and 1 μl of cDNA, in a total volume of 50 μl. The PCR conditions were 7 min at 94°C followed by 35 cycles of 94°C for 30 s, 55 to 58°C for 30 s, and 72°C for 1 min. RT-PCR products were separated by electrophoresis in 1% agarose gels and visualized by ethidium bromide staining under UV light.

Elimination of glycocalyx structures. The following enzymes were prepared in serum-free medium and were exposed to the apical surfaces of HAE prior to AdV inoculation under the indicated conditions: keratanase I and II (0.4 U/ml, 18 h; Seikagaku); *O*-sialoglycoprotein endopeptidase (120 mg/ml, 2 h; Cedarlane, Ontario, Canada); bovine testis hyaluronidase (1 mg/ml, 12 h; Worthington Biochemical Corporation); chondroitinase-4-sulfatase (160 mU/ml, 3 h; Seikagaku); chondroitinase ABC (0.5 U/ml, 3 h; Seikagaku); elastase (12 U/ml, 2 h; Sigma); heparinase I, II, or III (4 mIU/ml, 3 h; Sigma); heparinitinase (4 mIU/ml, 2 h; Sigma); protease XIV (0.01%, 2 h; Sigma); and neuraminidase III (160 mU/ml, 2 h; Sigma).

Metabolic inhibitors and vehicle controls were included in the basolateral medium 5 days prior to the exposure of HAE to AdVGFP or AdVLacZ. The following inhibitors were used: 1-deoxynojirimycin (1 mM), *N*-butyldeoxynojirimycin (1 mM), sodium chlorate (30 mM), and benzyl 2-acetamido-2-deoxy-α-D-galactopyranoside (1 mM) (all obtained from Sigma-Aldrich). In preliminary studies, the expression of AdVgpi-hCAR at the lumenal surface of HAE was not altered by a 5-day exposure to any of the enzymes or inhibitors used.

Freeze substitution and ruthenium red protocols. Human tracheal segments obtained according to UNC IRB-approved protocols were prepared for transmission electron microscopy (TEM) by the freeze substitution technique (see below) and were stored in liquid nitrogen (LN2). Airway epithelial cells were isolated from the same patient source used for the generation of HAE cultures, subjected to freeze substitution, and stored in LN2. Tissues and HAE samples were then processed and analyzed in parallel. For freeze substitution, samples were immersed in a cold 0.2 M sucrose solution (100 ml of 0.2 M Sorenson's buffer, 100 ml of distilled water, and 13.6 g of sucrose) for 1 h at 4°C. The samples were then immersed in a cold 25% glycerol solution (3.8 ml of 0.2 M Sorenson's buffer, 3.8 ml of distilled water, and 2.5 ml of glycerol) for no longer than 1 h, plunge frozen in Freon, and stored in LN2. The samples were transferred to cooled 4% osmium tetroxide in acetone, stored at −80°C for 4 days, and then transferred to −20°C for 2 h, 4°C for 2 h, and room temperature for 1 h. After an acetone wash, the samples were infiltrated with propylene oxide and embedded in Epon resin for standard TEM processing.

For the visualization of acid mucopolysaccharides of the glycocalyx layer, samples were immersed in a glutaraldehyde solution (5 ml of 4% glutaraldehyde, 5 ml of 0.2 M cacodylate buffer, and 1,500 ppm of ruthenium red) for 1 h at room temperature. After being rinsed in 0.2 M cacodylate buffer, the tissues were immersed in an osmium tetroxide solution (5 ml of 5% osmium tetroxide, 5 ml of 0.2 M cacodylate buffer, and 5 ml with 1,500 ppm of ruthenium red) for 3 h at room temperature. After a rinse in 0.2 M cacodylate buffer, standard processing for TEM was performed.

Analyses of glycocalyx abundance by TEM. Three different sections of isolated murine tracheas were obtained from $Muc1^{+/+}$ or $Muc1^{-/-}$ animals, and sections stained with ruthenium red were used to visualize the membrane glycocalyx by TEM (20). Electron photomicrographs were captured at a magnification of ×12,000, and the glycocalyx height associated with either nonciliated or ciliated membranes was measured via image processing as follows. Each image containing either a nonciliated or ciliated membrane was scanned into Adobe Photoshop, a threshold determination for the image was conducted to outline the ruthenium red-dense glycocalyx layer, and an "and" Boolean image process was applied. The depth of the ruthenium red staining was measured in terms of pixels, averaged, and converted into nanometers. The investigator who performed the analysis was blinded to the genotypes of the samples until after data analyses, and the number of images assessed for each section from each animal was >30.

RESULTS

Generation of human airway epithelial cell cultures expressing GPI-hCAR. Well-differentiated HAE cultures expressing GPI-hCAR (GPI-hCAR HAE) were generated by transducing columnar airway epithelial cells with AdVgpi-hCAR. It was previously shown that airway columnar cells are resistant to AdV transduction after inoculation of the lumenal surface (26, 28, 36, 47). We achieved a high level of gene transfer in HAE cultures by transiently disrupting epithelial cell tight junctions with sodium caprate (30 mM for 3 min, apical exposure) (16) to allow the exposure of basolateral endogenous hCAR to AdVGFP (2×10^{10} particles/ml for 2 h at 37°C; $\sim 4 \times 10^4$ PPC). For HAE cultures that were not treated with sodium caprate but were inoculated with lumenal AdVGFP, few epithelial cells were positive for GFP (<0.01%) postinoculation (Fig. 1A, panel i). However, after sodium caprate treatment, AdVGFP inoculation of the apical surface of HAE resulted in a significant number of GFP-positive epithelial cells, with >70% of the cells that were exposed to virus expressing GFP (Fig. 1A, panel ii). Confocal XZ optical sectioning revealed that cells expressing GFP were columnar and that the majority of GFP-positive cells also costained with an antibody for a cilial shaft protein (β-tubulin IV), suggesting that ciliated columnar cells were the predominant cell type transduced by AdVGFP (Fig. 1A, panel iii). The transduction of only occasional β-tubulin IV-negative columnar cells most likely reflects the predominance of ciliated cells in this HAE model. Basal cells that were positive for GFP were rarely detected, even after sodium caprate treatment.

Identical techniques were used for the inoculation of HAE with AdVgpi-hCAR. With antibodies to detect GPI-hCAR expression 48 h after AdVgpi-hCAR inoculation, most cells (>70%) were positive for GPI-hCAR in HAE that was treated with sodium caprate (Fig. 1A, panel v) but not in HAE that was not treated with sodium caprate (Fig. 1A, panel iv). Confocal

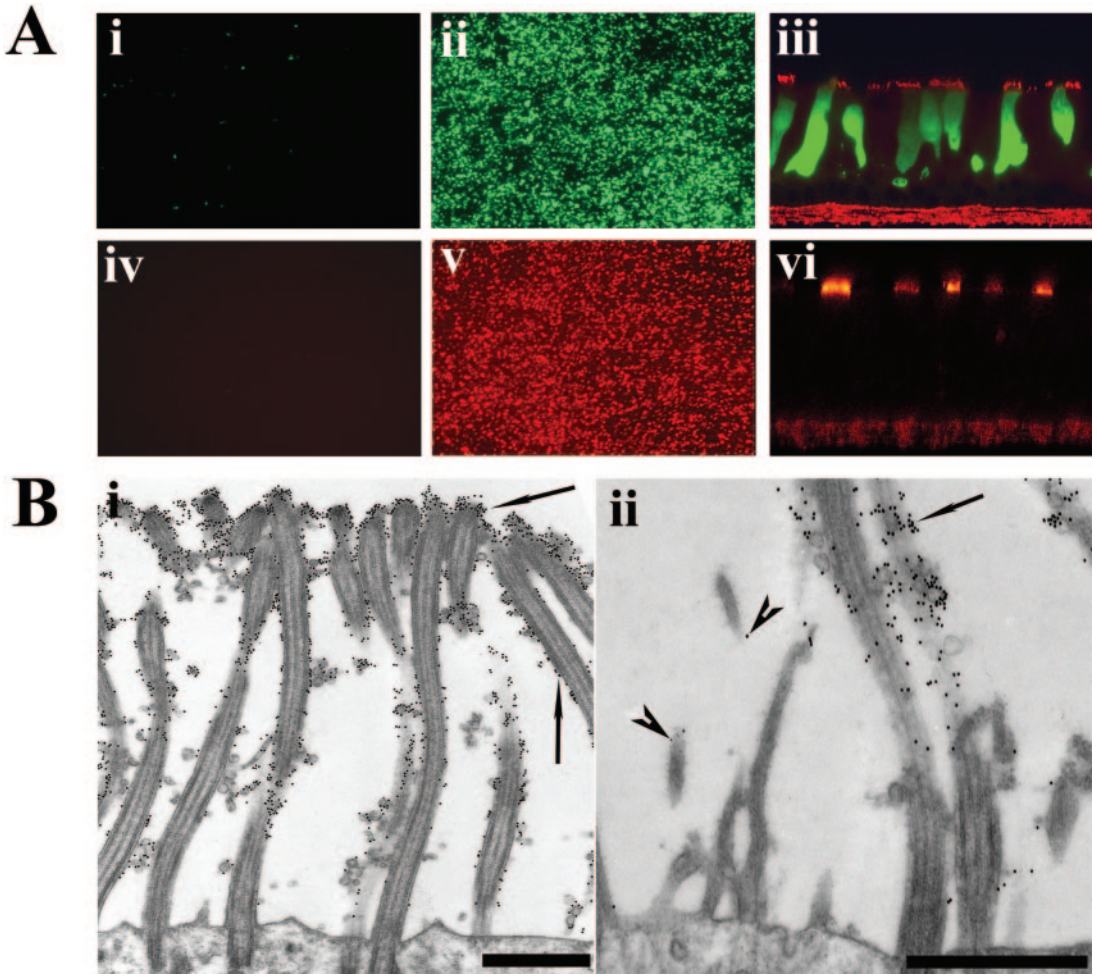

FIG. 1. AdV-mediated expression of GPI-hCAR in HAE and localization of GPI-hCAR to ciliated cell shafts. (A) Representative en face images of HAE inoculated with AdVGFP (i and ii) or AdVgpi-hCAR (iv and v) without (i and iv) or with (ii and v) disruption of epithelial tight junctions by sodium caprate, with gene expression being assessed 48 h later. Original magnification, ×10. Confocal XZ optical sectioning of HAE expressing GFP (green) and probed with anti-β-tubulin IV conjugated to Texas Red (red) indicated that predominately ciliated columnar epithelial cells were transduced by AdVGFP (iii), and GPI-hCAR expressed in HAE was localized to the apical surface, as detected by anti-hCAR (RmcB) conjugated to Texas Red (red) (vi). Original magnification, ×63. (B) Transmission electron micrographs of HAE inoculated with AdV-gpi-hCAR and probed with RmcB conjugated to immunogold particles (12-nm diameter) revealed that GPI-hCAR was predominately localized to the cilial shafts of ciliated cells (i, arrows), with less localization to the microvillus structures on ciliated cells (ii, arrowheads). HAE inoculated with AdVGFP or a vehicle control alone and probed with RmcB showed no immunogold labeling. Bar = 1 μm.

XZ optical sectioning determined that the localization of GPI-hCAR was at the lumenal surface (Fig. 1A, panel vi). Further analyses of GPI-hCAR localization in HAE by immunogold TEM detected GPI-hCAR on the lumenal surfaces of ciliated (Fig. 1B, panel i) and occasionally nonciliated cells (not shown). In ciliated cells, GPI-hCAR was detected on the cilial shafts, and to a lesser extent, on microvilli (Fig. 1B, panel ii).

Expression of apical surface GPI-hCAR does not significantly enhance gene transfer via the lumenal surface of HAE. To determine whether the expression of GPI-hCAR at the lumenal surface was sufficient for AdV-mediated gene transfer, we inoculated the apical surface of HAE (Fig. 2A, panel i) or GPI-hCAR HAE (Fig. 2A, panel ii) with AdVGFP (2×10^{10} particles/ml for 2 h at 37°C; $\sim 4 \times 10^4$ PPC) and assessed GFP expression 48 h later. For HAE, few cells (<0.05%) were positive for GFP after AdV inoculation, indicating a low gene transfer efficiency (Fig. 2A, panel iii). The inoculation of GPI-hCAR HAE with AdVGFP resulted in a modest improvement in gene transfer efficiency (~2% of the cells expressed GFP) (Fig. 2A, panel iv). However, a comparison of the number of GFP-positive cells with the number of cells expressing GPI-hCAR (>70%) showed that only 3% of GPI-hCAR-positive cells were transduced by AdVGFP. These data suggest that the majority of columnar cells expressing GPI-hCAR at the apical surface did not interact with AdVGFP in a manner that was conducive to gene transfer. Quantitative analyses using AdVLacZ (2×10^{10} or 2×10^{11} particles/ml) demonstrated that at best only a two- to threefold increase in gene transfer was achieved in the presence of GPI-hCAR, even when high inocula of AdV were used (Fig. 2B). These data suggest that AdV was unable to interact with GPI-hCAR localized on the apical surface or that this receptor was insufficient for mediating viral penetration into HAE. Since GPI-hCAR and hCAR were previously shown to mediate AdV-mediated gene trans-

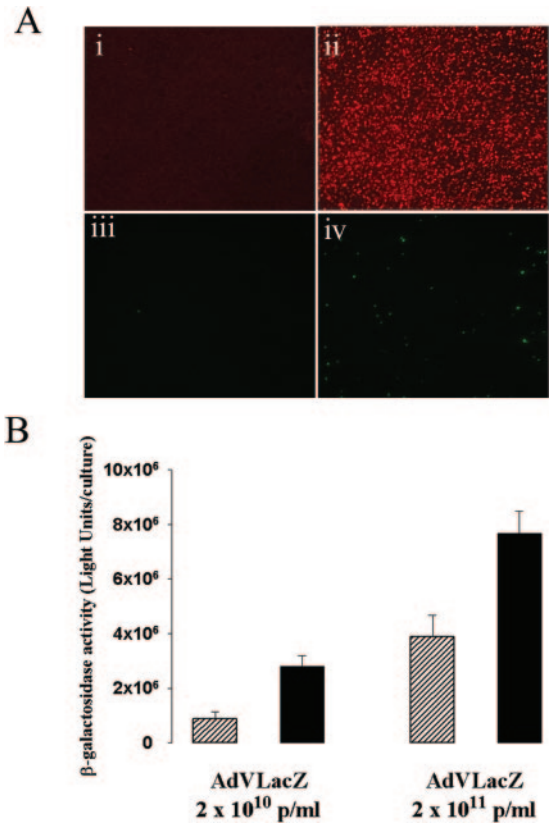

FIG. 2. Inefficient AdV-mediated gene transfer to HAE in the presence of apical GPI-hCAR. (A) Representative en face views of control HAE (i and iii) and GPI-hCAR HAE (ii and iv) either probed with anti-hCAR conjugated to Texas Red (i and ii) or monitored for GFP expression 48 h after inoculation with AdVGFP (iii and iv). Original magnification, ×10. (B) Quantitative LacZ enzymatic analyses of control HAE (hatched bars) or GPI-hCAR HAE (solid bars) 48 h after inoculation of the apical surfaces of the HAE cultures with AdVLacZ at 2×10^{10} or 2×10^{11} particles/ml. The data represent 14 samples for each bar from cultures derived from four different patient samples and are means ± standard errors (SE).

fer equally in nonpolarized cell lines (27, 34, 37), our data support the hypothesis that an extracellular barrier on the apical surface of HAE restricts AdV access to GPI-hCAR.

Identification of glycoconjugates on the HAE apical surface. To identify components of the HAE surface glycocalyx, we probed the apical surface with lectins and antibodies for specific glycoconjugates (Fig. 3). These data revealed that the apical surface of HAE is rich in α2-6-linked sialic acid residues (SNA probe) (Fig. 3, panel i) but not α2-3-linked sialic acid residues (MAL II probe) (Fig. 3, panel ii). The predominance of the α2-6 linkage of sialic acid on HAE is consistent with the large numbers of ciliated cells and the previous localization of this linkage to ciliated cell surfaces (3). The highly sialylated, O-glycosylated tethered mucin MUC1 was also abundant on the apical surface of HAE, as shown by use of a well-characterized MUC 1 antibody (b2729) (8, 9) (Fig. 3, panel iii).

Glycocalyx structures also often contain proteoglycans, the presence of which was evaluated by the use of antibodies for specific glycosaminoglycan chains. Keratan sulfate (KS) was detected at the apical surface of HAE, but only on subpopulations of cells (Fig. 3, panel iv). Members of our laboratory previously localized KS to the apical surfaces of ciliated cells in HAE (48). Immunoreactivity for heparan sulfate (Fig. 3, panel v), chondroitin-4- and -6-sulfate, and dermatan sulfate was not detected on the apical surface of HAE.

Disruption of apical surface glycocalyx structure as a strategy to increase AdV-mediated gene transfer. The identification of HAE glycocalyx components suggested strategies to eliminate this barrier in an attempt to improve the accessibility of AdV to GPI-hCAR. Preliminary experiments in which GPI-hCAR was pretreated with a broad-spectrum NA (NA III from *Vibrio cholerae*) did not enhance the AdV-mediated gene transfer efficiency (results not shown), indicating that the apical barrier on HAE did not solely involve sialic acid residues, as was found for MDCK cells (27). This suggested that the glycocalyx of HAE is more complex and/or more robust than that of MDCK cells. We tested whether the KS-degrading enzymes keratanase I and/or II could improve AdV-mediated gene transfer to GPI-hCAR HAE cultures. Although KS was efficiently cleaved from the apical surface (determined by the loss of 5D4 antibody immunoreactivity), AdV-mediated gene transfer was not enhanced (data not shown). Similarly, enzymatic reagents that specifically degraded heparan sulfate (heparinases), chondroitin sulfate (chondroitinase ABC), hyaluronan (hyaluronidase), and glycoproteins (*O*-sialoglycoprotein endopeptidase and elastase) all failed to improve gene transfer efficiency to GPI-hCAR HAE (data not shown). In contrast, the nonspecific protease XIV (PXIV) enhanced gene transfer efficiency to GPI-hCAR HAE six- to eightfold compared with that for HAE. PXIV pretreatment also resulted in a modest (two- to threefold) increase in gene transfer to a HAE culture that did not express GPI-hCAR (Fig. 4A).

Inhibitors of glycan synthesis were also tested to determine if reduced glycosylation of the cell surface could enhance the gene transfer efficiency. For these studies, HAE cultures were maintained in the presence of *N*-butyldeoxynojirimycin (a glycosphingolipid inhibitor), 1-deoxynojirimycin (an *N*-glycan synthesis inhibitor), sodium chlorate (an inhibitor of sulfation), or benzyl 2-acetamido-2-deoxy-α-D-galactopyranoside (a py-

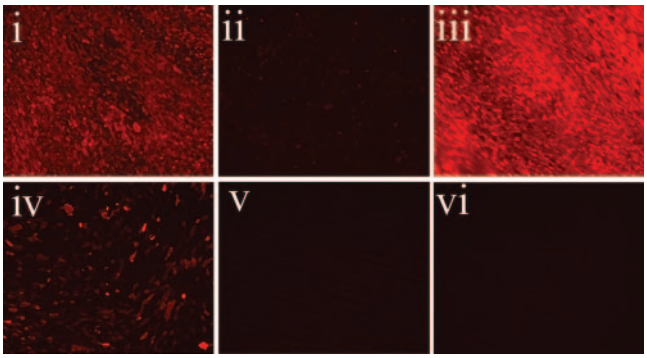

FIG. 3. Immunodetection of glycoconjugates on the apical surfaces of HAE cultures. Cultures were exposed to probes for the following: (i) α2-6-linked sialic acid residues, (ii) α2-3-linked sialic acid residues, (iii) MUC1 glycoprotein, (iv) keratan sulfate, and (v) heparan sulfate or chondroitin sulfate. The probes were then detected with secondary reagents conjugated to Cy3 or Texas Red. Secondary reagents in the absence of specific probes showed no fluorescence on HAE (vi). Original magnification, ×10.

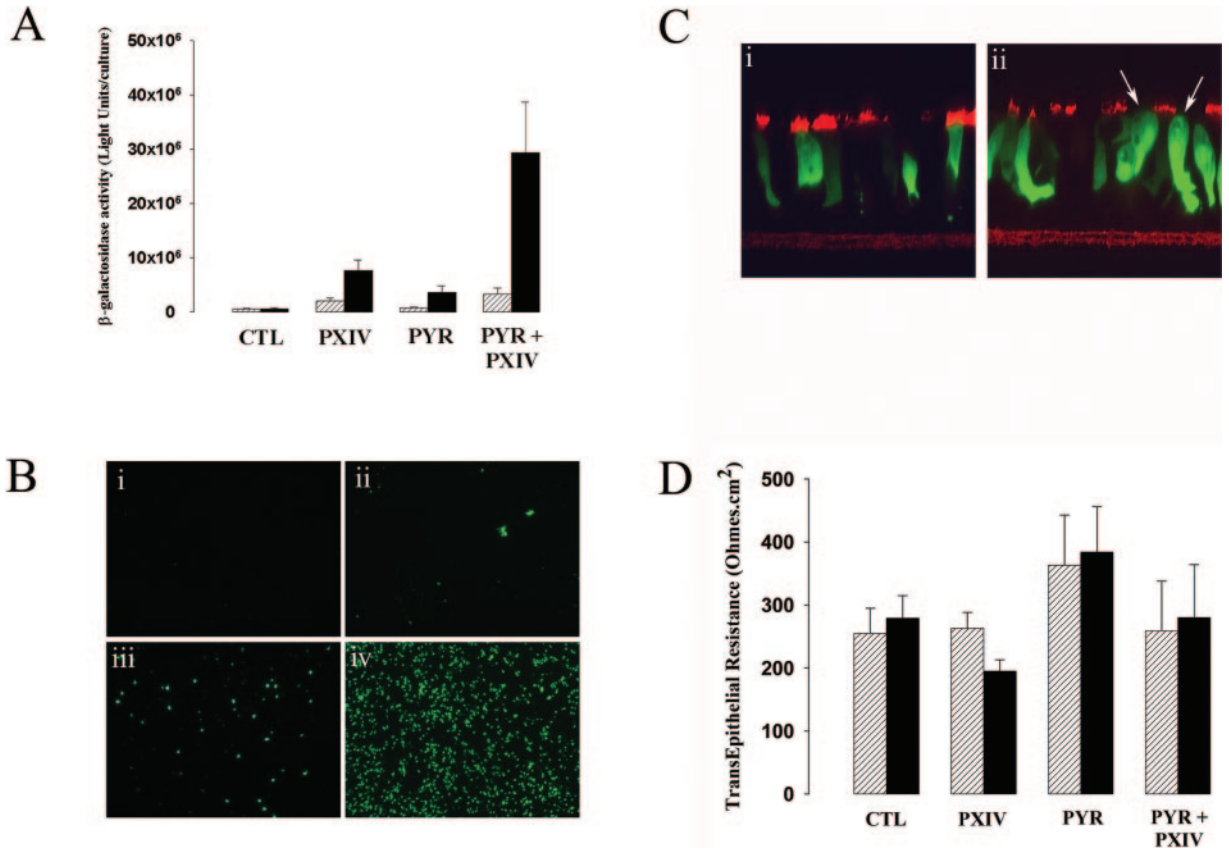

FIG. 4. Enhancement of AdV-mediated gene transfer to GPI-hCAR HAE after elimination of apical surface glycocalyx. (A) Quantitative LacZ enzyme analyses of AdV-mediated gene transfer 48 h after inoculation of HAE (hatched bars) or GPI-hCAR HAE (solid bars) either without treatment (CTL; $n = 5$ for each group) or after treatment of the apical surface with PXIV (0.01%; $n = 6$), PYR (5 mM; $n = 8$), or a combination of both reagents (PYR + PXIV; $n = 5$). Data represent means ± SE for two different patient samples. (B) Representative en face images of HAE (i and iii) and GPI-hCAR HAE (ii and iv) with no treatment (i and ii) and after apical surface treatment with a combination of PYR and PXIV (iii and iv). Original magnification, ×10. (C) Confocal XZ optical sectioning of GPI-hCAR HAE pretreated with PYR and PXIV, inoculated with AdVGFP, and assessed for GFP expression 48 h later. Colocalization with anti-hCAR conjugated to Texas Red (i) or anti-β-tubulin IV conjugated to Texas Red (ii) revealed that GFP-expressing cells also expressed GPI-hCAR and were predominately ciliated. The rare occurrence of GPI-hCAR-negative cells that were positive for GFP most likely reflected the absence of GPI-hCAR detection within the optical plane analyzed. Nonciliated cells were also occasionally positive for GFP expression (ii, arrows). Original magnification, ×63. (D) Effect of PYR and PXIV treatment on the TERs of HAE (hatched bars) and GPI-hCAR HAE (solid bars). Data represent means ± SE for at least five cultures from two different patient samples.

ranoside [PYR] that is an *O*-glycan inhibitor) for 5 days prior to the inoculation of HAE or GPI-hCAR HAE with AdV. None of the reagents affected HAE morphology, the beating of cilia, or the maintenance of an air-liquid interface during the 5 days of treatment. Of the reagents tested, only PYR modestly increased AdV-mediated gene transfer efficiency (Fig. 4A), suggesting that O-linked glycosylation provided at least a minor component of the apical surface barrier to AdV access.

Since we have hypothesized that the O-linked glycoproteins contribute significantly to the glycocalyx barrier, we assessed the effect of sequentially treating cultures with PYR for 5 days and then exposing the apical surfaces of HAE to PXIV. This strategy resulted in a synergistic improvement in AdV-mediated gene transfer, with a 30-fold increase in gene transfer for GPI-hCAR HAE compared to that achieved with untreated HAE (Fig. 4A and B). In contrast, PYR and PXIV pretreatment only modestly enhanced AdV-mediated gene transfer to HAE (Fig. 4A and B). Confocal XZ optical sectioning of GPI-hCAR HAE revealed that the GFP-positive cells were columnar cells that were also positive for GPI-hCAR (Fig. 4C, panel i). Ciliated, and to a lesser extent, nonciliated cell types were targeted by AdVGFP (Fig. 4C, panel ii).

Since improvements in gene transfer to columnar cells may also reflect a disruption of tight junctions, the transepithelial resistance (TER) was measured as an index of tight junctional permeability at the time of AdV inoculation. For both HAE and GPI-hCAR HAE, TER was not significantly different for cultures treated with PYR and PXIV versus vehicle controls alone (Fig. 4D), and pretreatment did not reduce TER to levels (30 to 50 $\Omega \cdot cm^2$) that permit AdV to access endogenous hCAR (16).

When combined, these data suggest that apical membrane O-glycosylated protease-sensitive components of the human airway glycocalyx account for at least a portion of the barrier function against AdV accessing apical receptors. Although our antibody data suggest that MUC1 is present in this barrier, several other tethered mucins could account for this O-glycosylated, protease-sensitive component of the glycocalyx. At the

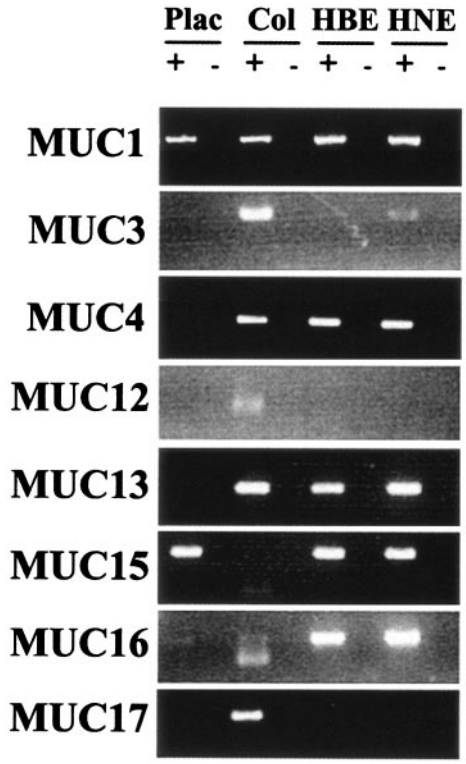

FIG. 5. RT-PCR analyses of human tethered mucin genes (MUC) in human placental (Plac), colon (Col), bronchial epithelial (HBE), and nasal epithelial (HNE) cells. + and −, RT-PCRs performed in the presence and absence, respectively, of reverse transcriptase.

present time, there are eight reported tethered mucins whose expression and function in the airway have not yet been defined. Using RT-PCR, we determined that the tethered mucin species MUC1, MUC4, MUC13, MUC15, and MUC16 are expressed in HAE, with no evidence for the expression of MUC12 and MUC17 (Fig. 5). At present, the contribution of each of the expressed mucin species to a glycocalyx barrier to AdV is unknown.

Comparison of glycocalyx abundance on human airway epithelium in vitro and in vivo. Although HAE cultures preserve many of the phenotypic characteristics of the human airway epithelium in vivo, i.e., ciliated and mucous cell differentiation, ion transport capacities, mucus secretion, and mucociliary transport (23, 24, 31), it is unknown whether the mass of glycocalyx on HAE in vitro reflects that present on the human tracheobronchial epithelium in vivo. Therefore, we compared the relative amounts of glycocalyx on HAE cultures to those on freshly excised human tracheobronchial airway specimens. Since glycocalyx composition and quantity may differ among individual donors, we assessed the glycocalyxes in freshly excised tracheobronchial tissue and HAE generated from cells derived from the same donor. In preliminary experiments, we determined that standard preparation techniques for TEM resulted in dehydration of the samples, producing a significant loss and/or collapse of the glycocalyx carbohydrate structure. As an alternative, we used the freeze substitution technique, which better preserves the hydrated form of the glycocalyx structure (20). Representative TEM photomicrographs of ciliated and mucus cell apical surface glycocalyxes on HAE and freshly excised tissues derived from the same donor after freeze substitution are shown in Fig. 6. With this technique, glycocalyxes were visualized as abundant masses on the apical surfaces of ciliated and nonciliated cell types and were predominately localized on microvilli. The combination of the extended structure of the microvillar processes and the glycocalyx present on the microvilli provided an effective barrier depth of approximately 3 to 4 μm, i.e., ~50% of the length of a fully extended cilium. Although the overall depth of the glycocalyx layer on HAE was similar to that observed on freshly excised tissue, the increased density of web- or matrix-like structures on freshly excised tissues suggested that the glycocalyx was more abundant in vivo. Thus, in vitro results seem likely to underestimate the contribution of the glycocalyx as a barrier to gene transfer.

Generation of in vivo model to evaluate AdV gene transfer to airway epithelium. To determine the influence of an in vivo glycocalyx barrier to AdV-mediated gene transfer, we generated a transgenic mouse model with GPI-hCAR expression specifically in epithelial cells. RT-PCRs to amplify tethered mucins from tracheal and lung samples of mice suggested that, as for humans, the mouse glycocalyx contains a variety of O-glycosylated high-molecular-weight proteins that may contribute to a barrier function (Fig. 7). The tethered mucins Muc1, Muc4, Muc13, and Muc16 were expressed in murine trachea and lung samples, consistent with the presence of these mucins in HAE. Sequences for the mouse homologues of MUC12, -15, and -17 are currently unavailable, so the expression of these mucins could not be determined. Nonetheless, the tethered mucins are likely important components of both human airway and murine airway epithelial glycocalyxes, suggesting that the murine tracheal epithelium provides a reasonable in vivo model to test our hypothesis that the glycocalyx provides a barrier to efficient gene transfer by restricting the access of AdV to receptors located on the apical surface. To develop our in vivo model, we generated transgenic mice expressing GPI-hCAR selectively in epithelial cells by using the epithelial cell-specific K18 promoter.

To determine whether the transgenic expression of GPI-hCAR led to apical surface localization in vivo, we probed airway regions from both transgenic and littermate control mice with a human CAR antibody (RmcB). All regions of transgenic mouse airways (nasal, tracheal, bronchial, and bronchiolar regions) were positive for GPI-hCAR. We detected GPI-hCAR expression throughout the airways of four different founder lines, although the expression levels were not consistent between lines. For further study, we chose a founder line that gave robust and consistent expression of GPI-hCAR in the airway epithelium. Figure 8 shows representative sections from transgenic murine nasal and lower airway epithelia displaying GPI-CAR expression predominately on the apical surfaces of the epithelia. RmcB immunoreactivity was not detected in any region of the airway epithelium derived from littermate controls. The submucosal glands of the murine nasal and tracheal epithelia were also positive for GPI-hCAR expression (Fig. 8, panel i). No RmcB immunoreactivity was detected in the alveolar regions (not shown).

In order to extend the model, we used the availability of Muc1 knockout mice ($Muc1^{-/-}$) to test the effect of removing

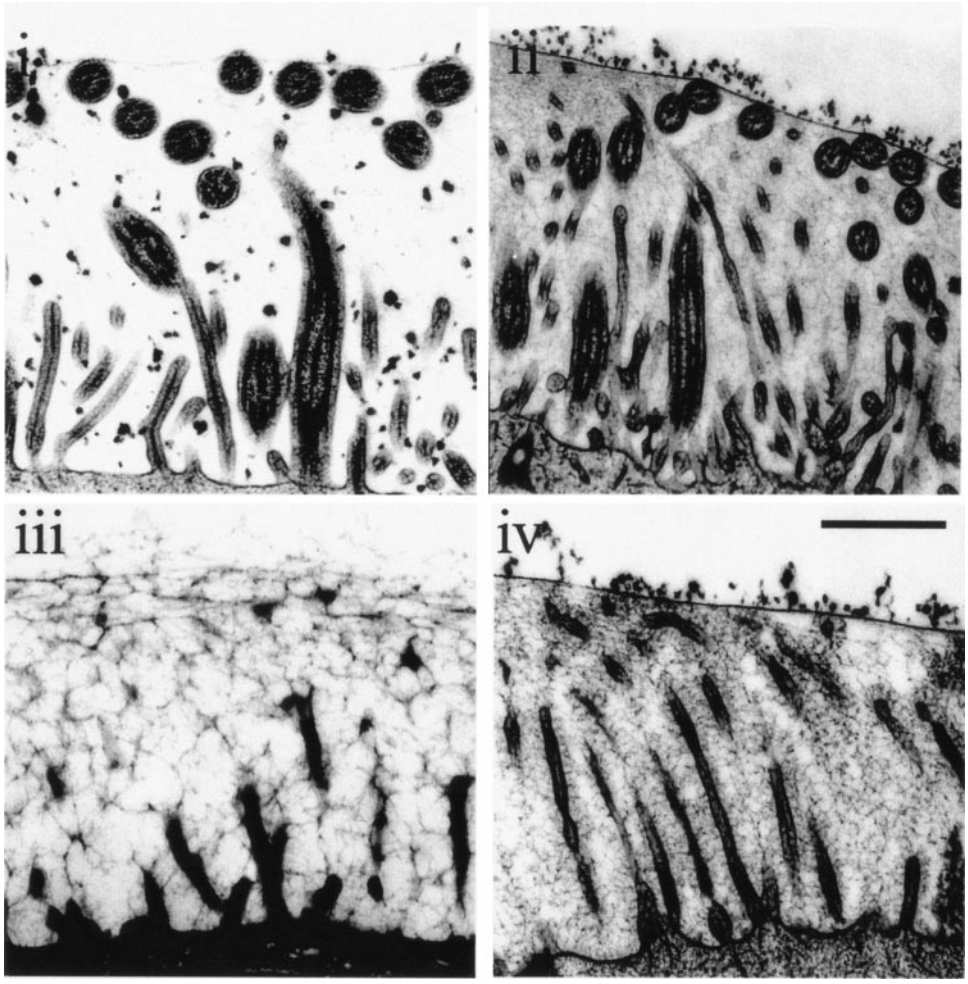

FIG. 6. Assessment of glycocalyx abundance on the surfaces of human airway epithelia in vitro and ex vivo by freeze substitution and transmission electron microscopy of HAE cultures (i and iii) and freshly excised human airway epithelium (ii and iv). Representative regions of the apical surfaces of ciliated cells (i and ii) and nonciliated cells that possess microvillus structures but not cilia are shown (iii and iv). Bar = 1 μm.

Muc1 on the AdV gene transfer efficiency in vivo. GPI-hCAR transgenic mice were bred to express GPI-hCAR with or without Muc1 and were maintained with homozygosity for Muc1 (+/+ or −/−) and heterozygosity at the transgenic GPI-hCAR locus. As described above, GPI-hCAR was localized to the apical surface of the tracheal epithelium in GPI-hCAR transgenics (Fig. 9A, panel i) but not in littermate controls (Fig. 9A, panel ii). In transgenic murine tracheas displaying GPI-CAR expression at the apical surface of the epithelium, Muc1 was localized to the tracheal epithelium, as visualized with an antibody (CT2) generated against the C-terminal domain of murine Muc1 (17). CT2 immunoreactivity was detected on the apical surface of the tracheal epithelium in GPI-hCAR/Muc1$^{+/+}$ mice but not GPI-hCAR/Muc1$^{-/-}$ mice (Fig. 9A, panels iv and vi, respectively). For Muc1$^{+/+}$ mice, CT2 immunoreactivity colocalized with RmcB immunoreactivity. Tracheal submucosal glands were the only airway regions that were positive for GPI-hCAR but not for Muc1 in GPI-hCAR/Muc1$^{+/+}$ mice (results not shown). In contrast, for GPI-hCAR/Muc1$^{+/+}$ transgenics, Muc1 expression but not GPI-hCAR expression was detected in type II alveolar epithelial cells (results not shown). With RmcB conjugated to immunogold particles, GPI-hCAR expression in the transgenic murine tracheal epithelium was localized to the apical surfaces of both ciliated and Clara cells (Fig. 9B). The distribution of GPI-hCAR to the cilial shafts and, to a lesser extent, the microvilli of murine ciliated cells resembled the distribution of GPI-hCAR in HAE in vitro.

Intralumenal delivery of AdV to murine tracheal epithelium in vivo. Since the controlled delivery of viral vectors to defined regions of the murine lung in vivo is difficult, we delivered AdV to the tracheal airway epithelium by using a previously described double-tracheostomy method (26). Representative en face images of tracheal epithelia from Muc1$^{+/+}$, GPI-hCAR/Muc1$^{+/+}$, Muc1$^{-/-}$, and GPI-hCAR/Muc1$^{-/-}$ mice inoculated with AdLacZ and processed for the visualization of LacZ expression 48 h later are shown in Fig. 10A. The inoculation of Muc1$^{+/+}$ (Fig. 10A, panel i) and GPI-CAR/Muc1$^{+/+}$ (Fig. 10A, panel ii) tracheal epithelia with AdVLacZ (10^{11} particles/ml, 20 μl for 0.5 h) resulted in few positive epithelial cells, with most positive regions being areas of epithelial injury secondary to surgery. In contrast, the inoculation of Muc1$^{-/-}$ (Fig. 10A, panel iii) and GPI-hCAR/Muc1$^{-/-}$ (Fig. 10A, panel iv) tracheas with AdV resulted in enhanced gene transfer. Longitu-

FIG. 7. RT-PCR analyses of murine tethered mucin genes (Muc) in the murine colon (Col), murine trachea (Trach), or murine whole lung (Lung). + and −, RT-PCRs performed in the presence and absence, respectively, of reverse transcriptase.

dinal histological cross sections of representative tissues from each group of animals revealed that ciliated and nonciliated cell types expressed LacZ in GPI-hCAR/Muc1$^{-/-}$ mice (Fig. 10A, panels v and vi). Quantitative analyses revealed that non-

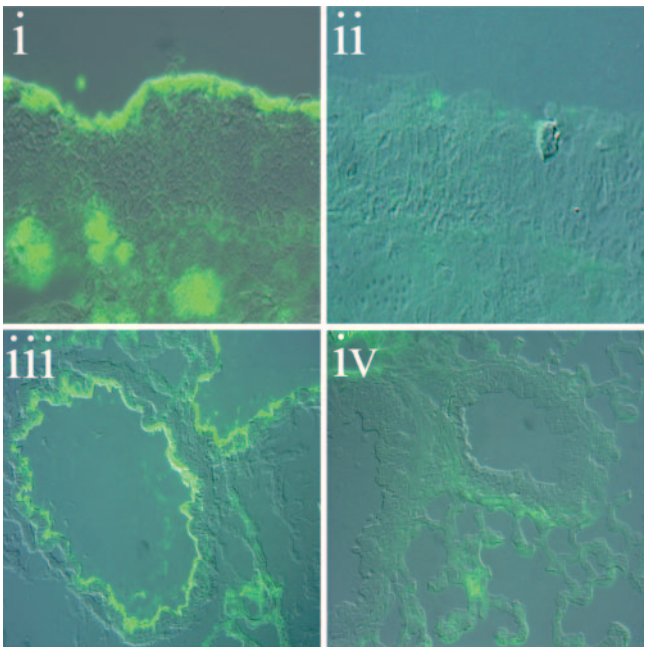

FIG. 8. Localization of RmcB immunoreactivity in the murine airway epithelium of K18-GPI-hCAR transgenic mice. Representative histological sections from murine nasal epithelia (i and ii) or small airway epithelia (iii and iv) derived from transgenics (i and iii) or littermate controls (ii and iv) and probed with RmcB and secondary antibodies conjugated to fluorescein isothiocyanate (green) are shown. Note that RmcB immunoreactivity below the surface of the nasal epithelium occurred in regions associated with glandular structures. Original magnification, ×100.

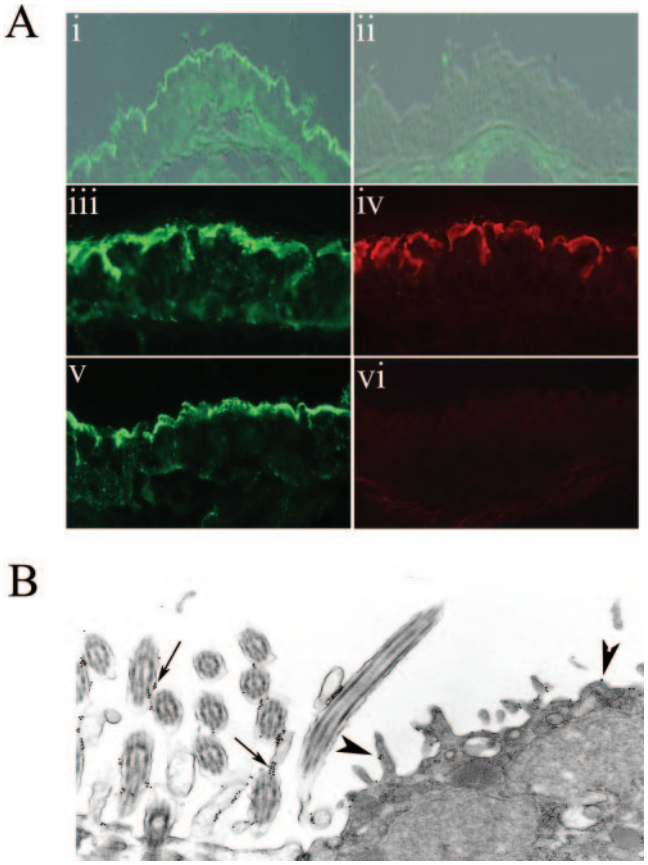

FIG. 9. Expression of GPI-hCAR and Muc1 glycoprotein at the apical surfaces of murine tracheal epithelia derived from GPI-hCAR transgenic mice. (A) Immunolocalization of GPI-hCAR (green) to the apical surfaces of murine tracheas derived from K18-GPI-hCAR transgenics (i) but not littermate controls (ii). The colocalization of GPI-hCAR (iii, green) and Muc1 (iv, red) in GPI-hCAR/Muc1$^{+/+}$ transgenic animals and the presence of GPI-hCAR (v, green) but not Muc1 (vi, red) at the apical surfaces of murine tracheal epithelia from GPI-hCAR/Muc1$^{-/-}$ animals are shown. Bar = 20 μm. (B) Electron micrographs of GPI-hCAR-expressing murine tracheal epithelium probed with anti-hCAR and detected with anti-mouse IgG conjugated to immunogold particles (12-nm diameter). Immunogold was detected on the cilial shafts of ciliated cells (arrows) and the apical surfaces of Clara cells (arrowheads). Similar procedures performed with a littermate control tracheal epithelium revealed no immunogold localization. Bar = 500 nm.

transgenic Muc1$^{+/+}$ control animals expressed LacZ in 1.6% ± 0.2% (range, 0.1 to 6.0%; n = 30) of the tracheal epithelial surface area, whereas GPI-hCAR/Muc1$^{+/+}$ mice expressed LacZ in 1.7% ± 0.3% (range, 0.0 to 6.0%; n = 30) of the tracheal epithelial surface area (Fig. 10B). These values were not statistically different, suggesting that the expression of an apical receptor in the tracheal epithelium in vivo was not sufficient to enhance AdV-mediated gene transfer.

However, there was an increase in gene transfer efficiency for mice in the Muc1$^{-/-}$ background for both nontransgenic and GPI-hCAR-positive animals. Quantitative image analyses (Fig. 10B) revealed that for Muc1$^{-/-}$ mice, AdV-mediated gene transfer increased to 4.9% ± 0.6% (range, 3.0 to 6.6%; n = 7) of the tracheal epithelial surface area. The presence of GPI-hCAR in Muc1$^{-/-}$ mice led to gene transfer in 7.9% ±

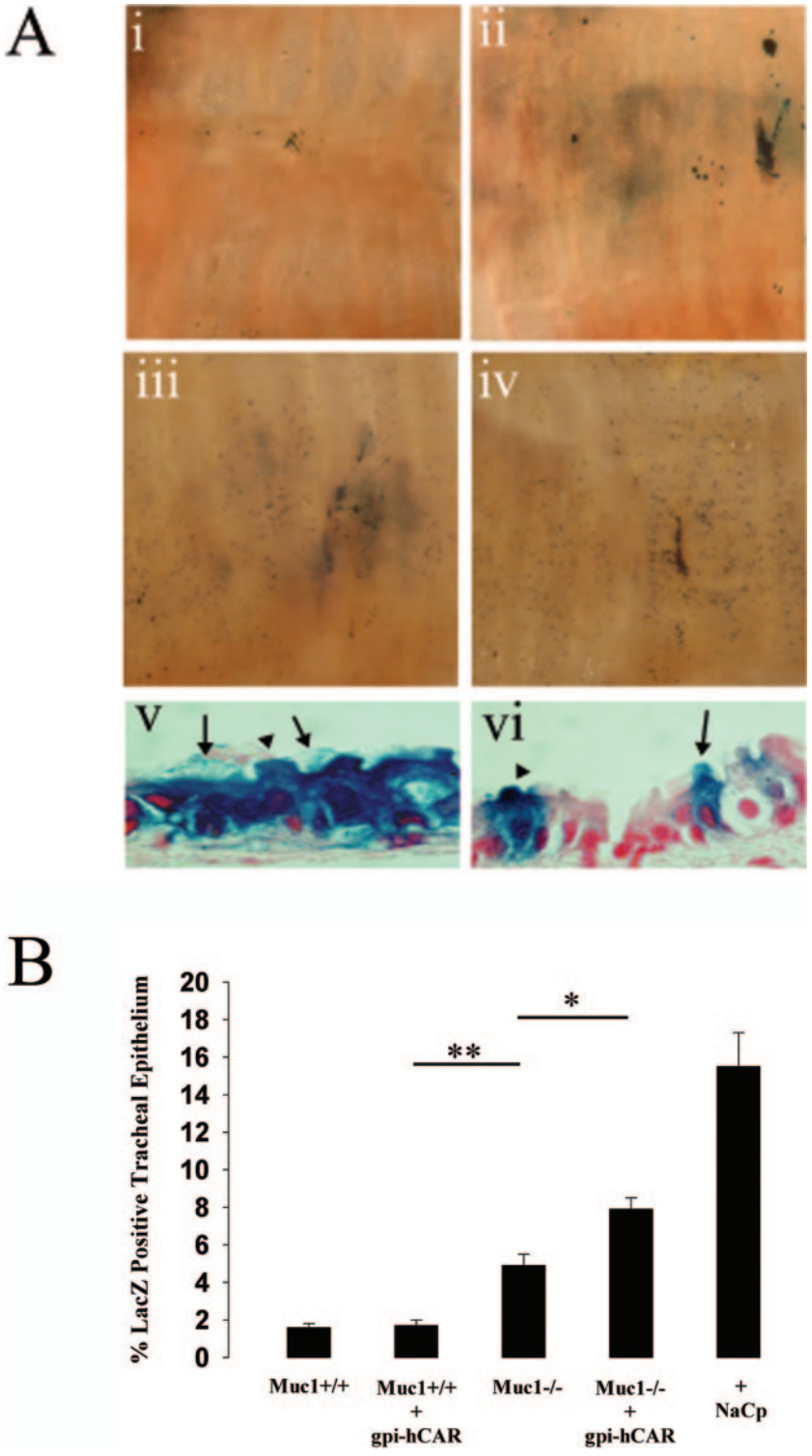

FIG. 10. AdV-mediated gene transfer to murine tracheal epithelium is enhanced by GPI-hCAR only in the absence of Muc1 glycoprotein from the lumenal surface. (A) Representative photomicrographs of excised murine tracheas displaying LacZ expression in the surface epithelium. Tracheal epithelia from control (i), GPI-hCAR transgenic (ii), Muc1$^{-/-}$ knockout (iii), and GPI-hCAR/Muc1$^{-/-}$ (iv) animals were inoculated with AdVLacZ (20 μl at 10^{11} particles/ml) and assessed 48 h later for gene transfer. Histological sections of murine tracheal epithelia from GPI-hCAR/Muc1$^{-/-}$ animals revealed that airway surface epithelial cells expressed the transgene, with both ciliated cells (v, arrows) and Clara cells (vi, arrows) being transduced by AdVLacZ. (B) Quantitative morphological analyses of the percentages of epithelial surface area exposed to AdVLacZ that expressed LacZ after 48 h for tracheas derived from Muc1$^{+/+}$ ($n = 30$), GPI-hCAR/Muc1$^{+/+}$ ($n = 30$), Muc1$^{-/-}$ ($n = 7$), and GPI-hCAR/Muc1$^{-/-}$ ($n = 22$) animals. For comparison, the percentage of epithelial surface area expressing LacZ after sodium caprate treatment (25 mM) prior to AdVLacZ inoculation is shown ($n = 12$). Data represent means ± SE. * and **, statistically significant differences, with $P < 0.0002$ and $P < 0.02$, respectively.

0.6% (range, 3.1 to 13.4%; $n = 22$) of the tracheal epithelial surface area. For comparison, AdV-mediated gene transfer immediately after tight junction disruption by a sodium caprate pretreatment (25 mM) resulted in 15.5% ± 1.8% (range, 7.1 to 23.6%; $n = 12$) of the tracheal epithelial surface area expressing LacZ. The percentages of tracheal epithelium that were transduced by AdVLacZ after sodium caprate pretreatment were not different when tracheas from control or GPI-CAR transgenic animals were used (not shown). Whether sodium caprate-facilitated gene transfer represents a maximum level of gene transfer efficiency with sodium caprate in this model or whether the efficiency of tight junctional disruption in vivo was significantly less than that achieved with sodium caprate in vitro remains to be determined.

These data suggest that Muc1 is one component of the murine tracheal epithelium glycocalyx that inhibits gene transfer. However, this molecule is not solely responsible for the barrier function of the glycocalyx, since AdV did not transduce all surface epithelial cells in the absence of Muc1.

Murine glycocalyx and the contribution of tethered Muc1 to this layer. Detection of the carbohydrate mass on the murine tracheal epithelium with ruthenium red revealed that both ciliated and nonciliated (Clara) cell types possessed an abundant apical surface glycocalyx (Fig. 11A). In addition to the microvillus surfaces being covered with the glycocalyx, the cilial shafts were also associated with significant ruthenium red staining, suggesting that a cilial glycocalyx layer may also function as a barrier to restrict AdV access to these regions. Further examination of the cilial shaft carbohydrate layer revealed that the glycocalyx was uniformly distributed along the shaft, with an estimated glycocalyx depth of ~50 nm. This measured depth is likely an underestimate since after TEM preparation the glycocalyx layer was significantly dehydrated and condensed with ruthenium red.

To estimate the contribution of Muc1 to this murine tracheal epithelium glycocalyx layer, we assessed the depths of the carbohydrate layers on tracheal epithelial cell surfaces of $Muc1^{+/+}$ and $Muc1^{-/-}$ mice by morphological analyses of the depth of ruthenium red staining (Fig. 11B). These data showed that the glycocalyx depth on the apical surfaces of nonciliated cells, but not on ciliated cells, was significantly reduced for $Muc1^{-/-}$ mice compared to the case for $Muc1^{+/+}$ mice. However, although differences in the overall glycocalyx depth were detected for $Muc1^{-/-}$ mice, the differences in depth represented only a fraction of the total depth. This finding suggests that although Muc1 is a component of the airway glycocalyx, other glycoconjugates contribute to this structure and the loss of a single mucin species will not dramatically alter the glycocalyx depth. The presence of other large, heavily glycosylated mucin species, as detected by RT-PCR, may account for the barrier function of the glycocalyx in the absence of MUC1/Muc1.

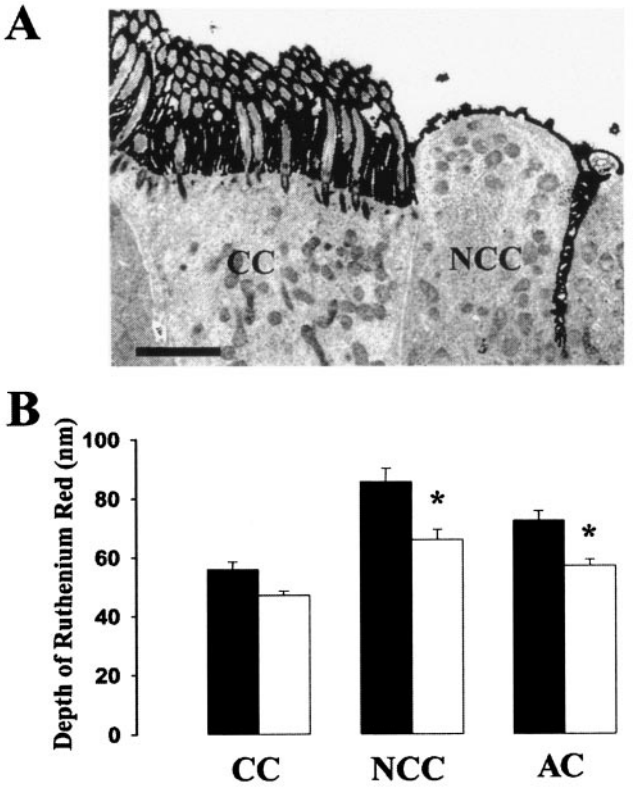

FIG. 11. Assessment of glycocalyx depth on the apical surface of murine tracheal epithelium in the presence and absence of Muc1 glycoprotein. (A) Representative transmission electron micrograph of murine tracheal epithelium stained with ruthenium red to assess the abundance of glycoconjugates. Ruthenium red staining on the apical surfaces of ciliated cells (CC) and nonciliated cells (Clara cell; NCC) is shown. Bar = 2 μm. (B) Quantitative morphological analyses of the depths of ruthenium red staining on the surfaces of ciliated cells (CC), nonciliated cells (NCC), or all cells (AC) of trachea epithelia derived from $Muc1^{+/+}$ (solid bars) and $Muc1^{-/-}$ (open bars) mice. The data shown represent means ± SE. *, statistically significant difference, with $P < 0.05$.

DISCUSSION

Studies of inefficient AdV-mediated gene transfer to the lumenal surfaces of well-differentiated human airway epithelial cells have previously focused on the absence of lumenal surface receptors that are required for AdV attachment and entry (CAR and α_V integrins) (28, 36, 47). These observations have led to strategies to retarget viral vectors to other apically located receptors that are competent for viral entry into the cell. By redirecting hCAR expression to the apical surfaces of the human tracheobronchial respiratory epithelium in vitro and the murine tracheal respiratory epithelium in vivo, we have tested the strategy of retargeting AdV to receptors on the lumenal surface and have shown that components of the airway surface glycocalyx restrict the access of AdV to these apical receptors. We have determined that O-glycosylated glycoprotein components of the airway glycocalyx, most likely tethered mucins such as MUC1, are major contributors to the barrier function of the glycocalyx structure. These findings suggest that strategies to retarget AdV to alternate receptor types present on the airway epithelial surface without methods to circumvent the glycocalyx barrier will have limited success. These observations may also have implications for AdV-mediated gene transfer strategies for cancer treatments since many epithelial cell cancers have been shown to overexpress tethered mucins on the cell surface, e.g., MUC1 in breast cancer (40), MUC4 in pancreatic cancer (2) and MUC16 in ovarian cancer (44).

The overall efficiency of gene transfer to HAE in vitro re-

mained low, with ~2 to 3% of cells being transduced by AdVGFP, despite the expression of a competent receptor at the apical surface (Fig. 2). In terms of CF lung disease applications, correction of the cyclic AMP-mediated chloride secretory response may require the expression of CFTR in ~10% of lumenal cells, whereas for sodium hyperabsorption correction, >80% of the cells must be transduced with CFTR (6). Therefore, to reach these levels with AdV, we must achieve improvements in gene transfer efficiency. Elimination of the glycocalyx barrier by the use of inhibitors of O-glycosylation and a nonspecific protease may provide a sufficient gene transfer efficiency for HAE in vitro; however, it is unlikely that sufficient elimination of the glycocalyx can be achieved to increase the gene transfer efficiency with retargeted AdV in vivo.

Compared to HAE in vitro, freshly excised human airway tissue also possessed a robust glycocalyx, suggesting that the restriction of AdV access would also be observed with human airways in vivo (Fig. 6). This was tested functionally with GPI-hCAR mouse tracheal epithelium in vivo, which confirmed that a glycocalyx barrier restricted AdV gene transfer in vivo (Fig. 10). Although it is difficult to directly compare the HAE model and the murine tracheal model since GPI-hCAR may be expressed at different levels in the two models and since human adenoviruses may not replicate as efficiently in murine airway cells as they do in human airway cells, these observations do suggest that the glycocalyx structure and abundance in vivo may provide a larger barrier to AdV than the glycocalyx layer of HAE cultures in vitro. This conclusion predicts that efforts to eliminate the glycocalyx layer in vivo by enzymatic means may be insufficient to improve the AdV-mediated gene transfer efficiency. Furthermore, inhibitors of O-glycosylation that are useful for in vivo delivery are not yet available.

The human airway glycocalyx is complex, with the large O-glycosylated mucin glycoproteins being a major component. The human airway epithelium expresses multiple mucin molecules, some of which are secreted mucins (e.g., MUC5AC and MUC5B), while others are tethered to the apical surface of the airway (e.g., MUC1 and MUC4). Given that MUC4 and MUC16 appear to be relatively highly expressed and that they are both large, heavily glycosylated tethered mucins (>1 MDa), it seems reasonable to speculate that these mucins, in addition to MUC1, have important barrier functions against infection of the airway epithelium by viruses such as AdV. The identification of MUC1 on the apical surface of HAE suggested that MUC1 is an important tethered mucin in HAE (Fig. 3). Strategies to specifically reduce the MUC1 abundance on HAE in vitro are not yet feasible, but the availability of a $Muc1^{-/-}$ mouse model allowed us to test the implications of removing Muc1 from the tracheal epithelium in vivo. The modest increase in AdV-mediated gene transfer observed in GPI-hCAR/$Muc1^{-/-}$ mice compared to nontransgenic $Muc1^{+/+}$ mice suggested a role for Muc1 in restricting AdV access. A surprising finding was the enhanced gene transfer observed in vivo for mouse tracheal epithelium that was devoid of both Muc1 and GPI-hCAR expression. These data suggest that the absence of Muc1 allowed gene transfer via a CAR-independent pathway, assuming that tight junctional integrity was not altered in the $Muc1^{-/-}$ mice. These observations are consistent with an earlier study in which the low level of CAR-independent AdV-mediated gene transfer to polarized MDCK cells was abolished by the transfection of MUC1 into these cells (1).

We have shown that GPI-hCAR was expressed in both ciliated and nonciliated cell types in HAE in vitro and in the mouse tracheal epithelium in vivo. Interestingly, GPI-hCAR was expressed in the shafts of ciliated cells in both species. These observations indicate that GPI-hCAR and possibly other GPI-linked proteins may have a tendency to localize to the cilial shaft membranes. Paramecium primary cilia contain proteins that are exclusively GPI-linked, suggesting that GPI-linked proteins favor the membrane environment of cilial structures (10).

Our in vitro data for HAE contrast with the results of a previous study that used a similar human airway epithelial cell culture model expressing GPI-hCAR at the lumenal surface (37). In the earlier report, apical GPI-hCAR expression was sufficient to mediate gene transfer to HAE, and the access of AdV to GPI-hCAR was unhindered by glycocalyx components. In our study, the improvement in gene transfer efficiency was low, with only 2 to 3% of GPI-hCAR-positive cells being transduced by AdVGFP. Although the reasons for the differences between these two studies are not immediately obvious, it is possible that they are due to the different culture conditions used for HAE. The cultures used for the present study were maintained in tissue culture medium supplemented with bovine pituitary gland extract, whereas in the previous study, Walters et al. used UltraSer G as a serum substitute. Although both culture conditions produce well-differentiated and ciliated HAE cultures, it is possible that the composition and/or abundance of the glycocalyx differed between the two HAE models. Interestingly, AdV has been shown to infect HeLa cells more efficiently when they are grown in UltraSer G than when they are grown in fetal bovine serum, an effect attributed to the increased access of AdV to cell surface receptors by a reduction in the steric hindrance of glycocalyx components (5). Our in vivo observations with a murine tracheal epithelium model also support our observations with HAE and indicate that the AdV-mediated gene transfer efficiency was not increased by GPI-hCAR expression. These data suggest that the glycocalyx provided an absolute barrier to AdV in vivo and that the in vitro HAE model may underestimate the restrictive nature of the glycocalyx to AdV in vivo.

The largely negative results with glycocalyx-degrading enzymes in our study and the ineffectiveness of *N*- and *O*-glycanase in an earlier study (37) may reflect the fact that these enzymes only affect specific carbohydrate linkages, leading to fragmented digestion of the large, heavily glycosylated molecules that remain restrictive to AdV. Indeed, our data indicate that the removal of sugar residues per se may not be sufficient to significantly improve gene transfer. The removal of proteinaceous structures by proteases to cleave the major portion of these molecules may be necessary to significantly improve gene transfer.

The glycocalyx layer may restrict AdV access to the apical surface by acting as a molecular sieve or by providing false substrates for AdV attachment. In earlier work, members of our laboratory used TEM to show that AdV was predominately associated with fine filamentous structures radiating from microvillus structures on human airway epithelial cells (28). These structures were likely components of the airway

glycocalyx. The fate of AdV attached to glycocalyx structures on the HAE cultures was not determined in this study. However, it has been shown with the murine airway that early after AdV administration to the lung, macrophages migrate to and internalize AdV particles that are present in the airway lumen attached to glycocalyx structures (49). It has been estimated that 70 to 90% of AdV particles are sequestered by airway macrophages 24 h after intralumenal administration to the lung (41, 49). We predict that glycocalyx components present AdV to incoming macrophages for phagocytosis and degradation. In addition to serving a presentation role, the tethered mucins are shed from the airway surface and incorporated into the soluble mucin layers (25). This feature raises the possibility that AdV attached to shed tethered mucins may be eliminated from airways by incorporation into the mucociliary transport system.

The difficulties of delivering AdV to the lumenal surfaces of human airways suggest that we consider other methods for delivering genes to the lung. Other viruses are known to efficiently infect the respiratory epithelium and have presumably evolved strategies to circumvent the glycocalyx barrier. Human coronaviruses, filoviruses, respiratory syncytial virus, and Sendai virus have improved gene transfer capacities for the airway epithelium after lumenal delivery compared to AdV (29, 38, 45, 48). Further studies of the interactions of these enveloped viruses with the airway epithelium and a definition of how they circumvent the glycocalyx barrier may reveal mechanisms that will aid the development of improved vectors for the delivery of therapeutic transgenes to the lung epithelium.

ACKNOWLEDGMENTS

This work was supported by NIH/NHLBI HL grants 51818-09 and HL 66943-01 and by the Cystic Fibrosis Research Foundation via a research grant (R.J.P.) and a summer studentship grant (R.W.L.).

We thank the directors and teams of the UNC CF Center Tissue Culture Core, the Molecular Core, the Morphology and Morphometry Core, and the Gene Therapy Vector Core and the staff of the Michael Hooker Microscopy Facility.

REFERENCES

1. **Arcasoy, S. M., J. Latoche, M. Gondor, S. C. Watkins, R. A. Henderson, R. Hughey, O. J. Finn, and J. M. Pilewski.** 1997. MUC1 and other sialoglycoconjugates inhibit adenovirus-mediated gene transfer to epithelial cells. Am. J. Respir. Cell Mol. Biol. **17:**422–435.
2. **Balague, C., G. Gambus, C. Carrato, N. Porchet, J. P. Aubert, Y. S. Kim, and F. X. Real.** 1994. Altered expression of MUC2, MUC4, and MUC5 mucin genes in pancreas tissues and cancer cell lines. Gastroenterology **106:**1054–1061.
3. **Baum, L. G., and J. C. Paulson.** 1990. Sialyloligosaccharides of the respiratory epithelium in the selection of human influenza virus receptor specificity. Acta Histochem. **40**(Suppl.)**:**35–38.
4. **Bergelson, J. M., J. A. Cunningham, G. Droguett, E. A. Kurt-Jones, A. Krithivas, J. S. Hong, M. S. Horwitz, R. L. Crowell, and R. W. Finberg.** 1997. Isolation of a common receptor for coxsackie B viruses and adenoviruses 2 and 5. Science **275:**1320–1323.
5. **Blixt, Y.** 1993. Exchange of the cellular growth medium supplement from fetal bovine serum to Ultroser G increases the affinity of adenovirus for HeLa cells. Arch. Virol. **129:**251–263.
6. **Boucher, R. C.** 1996. Current status of CF gene therapy. Trends Genet. **12:**81–84.
7. **Boucher, R. C.** 1999. Status of gene therapy for cystic fibrosis lung disease. J. Clin. Investig. **103:**441–445.
8. **Cao, Y., and U. Karsten.** 2001. Binding patterns of 51 monoclonal antibodies to peptide and carbohydrate epitopes of the epithelial mucin (MUC1) on tissue sections of adenolymphomas of the parotid (Warthin's tumours): role of epitope masking by glycans. Histochem. Cell Biol. **115:**349–356.
9. **Cao, Y., U. Karsten, and J. Hilgers.** 1998. Immunohistochemical characterization of a panel of 56 antibodies with normal human small intestine, colon, and breast tissues. Tumour Biol. **19:**88–99.
10. **Capdeville, Y., and A. Benwakrim.** 1996. The major ciliary membrane proteins in Paramecium primaurelia are all glycosylphosphatidylinositol-anchored proteins. Eur. J. Cell Biol. **70:**339–346.
11. **Chirmule, N., J. V. Hughes, G. P. Gao, S. E. Raper, and J. M. Wilson.** 1998. Role of E4 in eliciting CD4 T-cell and B-cell responses to adenovirus vectors delivered to murine and nonhuman primate lungs. J. Virol. **72:**6138–6145.
12. **Chow, Y. H., H. O'Brodovich, J. Plumb, Y. Wen, K. J. Sohn, Z. Lu, F. Zhang, G. L. Lukacs, A. K. Tanswell, C. C. Hui, M. Buchwald, and J. Hu.** 1997. Development of an epithelium-specific expression cassette with human DNA regulatory elements for transgene expression in lung airways. Proc. Natl. Acad. Sci. USA **94:**14695–14700.
13. **Chow, Y. H., J. Plumb, Y. Wen, B. M. Steer, Z. Lu, M. Buchwald, and J. Hu.** 2000. Targeting transgene expression to airway epithelia and submucosal glands, prominent sites of human CFTR expression. Mol. Ther. **2:**359–367.
14. **Chung, J. H., M. Whiteley, and G. Felsenfeld.** 1993. A 5′ element of the chicken beta-globin domain serves as an insulator in human erythroid cells and protects against position effect in Drosophila. Cell **74:**505–514.
15. **Cohen, C. J., J. T. Shieh, R. J. Pickles, T. Okegawa, J. T. Hsieh, and J. M. Bergelson.** 2001. The coxsackievirus and adenovirus receptor is a transmembrane component of the tight junction. Proc. Natl. Acad. Sci. USA **98:**15191–15196.
16. **Coyne, C. B., M. M. Kelly, R. C. Boucher, and L. G. Johnson.** 2000. Enhanced epithelial gene transfer by modulation of tight junctions with sodium caprate. Am. J. Respir. Cell Mol. Biol. **23:**602–609.
17. **Croce, M. V., M. T. Isla-Larrain, C. E. Rua, M. E. Rabassa, S. J. Gendler, and A. Segal-Eiras.** 2003. Patterns of MUC1 tissue expression defined by an anti-MUC1 cytoplasmic tail monoclonal antibody in breast cancer. J. Histochem. Cytochem. **51:**781–788.
18. **Drapkin, P. T., C. R. O'Riordan, S. M. Yi, J. A. Chiorini, J. Cardella, J. Zabner, and M. J. Welsh.** 2000. Targeting the urokinase plasminogen activator receptor enhances gene transfer to human airway epithelia. J. Clin. Investig. **105:**589–596.
19. **Grubb, B. R., R. J. Pickles, H. Ye, J. R. Yankaskas, R. N. Vick, J. F. Engelhardt, J. M. Wilson, L. G. Johnson, and R. C. Boucher.** 1994. Inefficient gene transfer by adenovirus vector to cystic fibrosis airway epithelia of mice and humans. Nature **371:**802–806.
20. **Hayat, M. A.** 1989. Principles and techniques of electron microscopy. CRC Press Inc., Boca Raton, Fla.
21. **Knowles, M. R., K. W. Hohneker, Z. Zhou, J. C. Olsen, T. L. Noah, P. C. Hu, M. W. Leigh, J. F. Engelhardt, L. J. Edwards, K. R. Jones, et al.** 1995. A controlled study of adenoviral-vector-mediated gene transfer in the nasal epithelium of patients with cystic fibrosis. N. Engl. J. Med. **333:**823–831.
22. **Kreda, S. M., R. J. Pickles, E. R. Lazarowski, and R. C. Boucher.** 2000. G-protein-coupled receptors as targets for gene transfer vectors using natural small-molecule ligands. Nat. Biotechnol. **18:**635–640.
23. **Matsui, H., B. R. Grubb, R. Tarran, S. H. Randell, J. T. Gatzy, C. W. Davis, and R. C. Boucher.** 1998. Evidence for periciliary liquid layer depletion, not abnormal ion composition, in the pathogenesis of cystic fibrosis airways disease. Cell **95:**1005–1015.
24. **Matsui, H., S. H. Randell, S. W. Peretti, C. W. Davis, and R. C. Boucher.** 1998. Coordinated clearance of periciliary liquid and mucus from airway surfaces. J. Clin. Investig. **102:**1125–1131.
25. **McNeer, R. R., D. Huang, N. L. Fregien, and K. L. Carraway.** 1998. Sialomucin complex in the rat respiratory tract: a model for its role in epithelial protection. Biochem. J. **330:**737–744.
26. **Pickles, R. J., P. M. Barker, H. Ye, and R. C. Boucher.** 1996. Efficient adenovirus-mediated gene transfer to basal but not columnar cells of cartilaginous airway epithelia. Hum. Gene Ther. **7:**921–931.
27. **Pickles, R. J., J. A. Fahrner, J. M. Petrella, R. C. Boucher, and J. M. Bergelson.** 2000. Retargeting the coxsackievirus and adenovirus receptor to the apical surface of polarized epithelial cells reveals the glycocalyx as a barrier to adenovirus-mediated gene transfer. J. Virol. **74:**6050–6057.
28. **Pickles, R. J., D. McCarty, H. Matsui, P. J. Hart, S. H. Randell, and R. C. Boucher.** 1998. Limited entry of adenovirus vectors into well-differentiated airway epithelium is responsible for inefficient gene transfer. J. Virol. **72:**6014–6023.
29. **Sinn, P. L., M. A. Hickey, P. D. Staber, B. L. Davidson, D. A. Sanders, and P. B. McCray, Jr.** 2001. Pseudotyping feline immunodeficiency virus (FIV) with a filovirus glycoprotein improves apical gene transfer to differentiated human airway epithelia. Pediatr. Pulmonol. **22**(Suppl.)**:**244.
30. **Spicer, A. P., G. J. Rowse, T. K. Lidner, and S. J. Gendler.** 1995. Delayed mammary tumor progression in Muc-1 null mice. J. Biol. Chem. **270:**30093–30101.
31. **Tarran, R., B. R. Grubb, D. Parsons, M. Picher, A. J. Hirsh, C. W. Davis, and R. C. Boucher.** 2001. The CF salt controversy. In vivo observations and therapeutic approaches. Mol. Cell **8:**149–158.
32. **Tomko, R. P., R. Xu, and L. Philipson.** 1997. HCAR and MCAR: the human and mouse cellular receptors for subgroup C adenoviruses and group B coxsackieviruses. Proc. Natl. Acad. Sci. USA **94:**3352–3356.
33. **Trapnell, B. C., and T. P. Shanley.** 2002. Innate immune responses to in vivo adenovirus infection, p. 349–373. *In* D. T. Curiel and J. T. Douglas (ed.), Adenoviral vectors for gene therapy. Academic Press, San Diego, Calif.

34. **van't Hof, W., and R. G. Crystal.** 2001. Manipulation of the cytoplasmic and transmembrane domains alters cell surface levels of the coxsackie-adenovirus receptor and changes the efficiency of adenovirus infection. Hum. Gene Ther. **12:**25–34.
35. **Walters, R. W., P. Freimuth, T. O. Moninger, I. Ganske, J. Zabner, and M. J. Welsh.** 2002. Adenovirus fiber disrupts CAR-mediated intercellular adhesion allowing virus escape. Cell **110:**789–799.
36. **Walters, R. W., T. Grunst, J. M. Bergelson, R. W. Finberg, M. J. Welsh, and J. Zabner.** 1999. Basolateral localization of fiber receptors limits adenovirus infection from the apical surface of airway epithelia. J. Biol. Chem. **274:** 10219–10226.
37. **Walters, R. W., W. van't Hof, S. M. Yi, M. K. Schroth, J. Zabner, R. G. Crystal, and M. J. Welsh.** 2001. Apical localization of the coxsackie-adenovirus receptor by glycosyl-phosphatidylinositol modification is sufficient for adenovirus-mediated gene transfer through the apical surface of human airway epithelia. J. Virol. **75:**7703–7711.
38. **Wang, G., C. Deering, M. Macke, J. Shao, R. Burns, D. M. Blau, K. V. Holmes, B. L. Davidson, S. Perlman, and P. B. McCray, Jr.** 2000. Human coronavirus 229E infects polarized airway epithelia from the apical surface. J. Virol. **74:**9234–9239.
39. **Wang, Y., F. J. DeMayo, S. Y. Tsai, and B. W. O'Malley.** 1997. Ligand-inducible and liver-specific target gene expression in transgenic mice. Nat. Biotechnol. **15:**239–243.
40. **Wolman, S. R., R. J. Pauley, A. N. Mohamed, P. J. Dawson, D. W. Visscher, and F. H. Sarkar.** 1992. Genetic markers as prognostic indicators in breast cancer. Cancer **70:**1765–1774.
41. **Worgall, S., G. Wolff, E. Falck-Pedersen, and R. G. Crystal.** 1997. Innate immune mechanisms dominate elimination of adenoviral vectors following in vivo administration. Hum. Gene Ther. **8:**37–44.
42. **Yang, Y., F. A. Nunes, K. Berencsi, E. E. Furth, E. Gonczol, and J. M. Wilson.** 1994. Cellular immunity to viral antigens limits E1-deleted adenoviruses for gene therapy. Proc. Natl. Acad. Sci. USA **91:**4407–4411.
43. **Yang, Y., Q. Su, and J. M. Wilson.** 1996. Role of viral antigens in destructive cellular immune responses to adenovirus vector-transduced cells in mouse lungs. J. Virol. **70:**7209–7212.
44. **Yin, B. W., and K. O. Lloyd.** 2001. Molecular cloning of the CA125 ovarian cancer antigen: identification as a new mucin, MUC16. J. Biol. Chem. **276:** 27371–27375.
45. **Yonemitsu, Y., C. Kitson, S. Ferrari, R. Farley, U. Griesenbach, D. Judd, R. Steel, P. Scheid, J. Zhu, P. K. Jeffery, A. Kato, M. K. Hasan, Y. Nagai, I. Masaki, M. Fukumura, M. Hasegawa, D. M. Geddes, and E. W. Alton.** 2000. Efficient gene transfer to airway epithelium using recombinant Sendai virus. Nat. Biotechnol. **18:**970–973.
46. **Zabner, J., L. A. Couture, A. E. Smith, and M. J. Welsh.** 1994. Correction of cAMP-stimulated fluid secretion in cystic fibrosis airway epithelia: efficiency of adenovirus-mediated gene transfer in vitro. Hum. Gene Ther. **5:**585–593.
47. **Zabner, J., P. Freimuth, A. Puga, A. Fabrega, and M. J. Welsh.** 1997. Lack of high affinity fiber receptor activity explains the resistance of ciliated airway epithelia to adenovirus infection. J. Clin. Investig. **100:**1144–1149.
48. **Zhang, L., M. E. Peeples, R. C. Boucher, P. L. Collins, and R. J. Pickles.** 2002. Respiratory syncytial virus infection of human airway epithelial cells is polarized, specific to ciliated cells, and without obvious cytopathology. J. Virol. **76:**5654–5666.
49. **Zsengeller, Z., K. Otake, S. A. Hossain, P. Y. Berclaz, and B. C. Trapnell.** 2000. Internalization of adenovirus by alveolar macrophages initiates early proinflammatory signaling during acute respiratory tract infection. J. Virol. **74:**9655–9667.